Geochemical Perspectives Letters

Ancient mantle plume components constrained by tungsten isotope variability in arc lavas

N. Messling[1*], G. Wörner[1], M. Willbold[1]

OPEN ACCESS

https://doi.org/10.7185/geochemlet.2321

Abstract

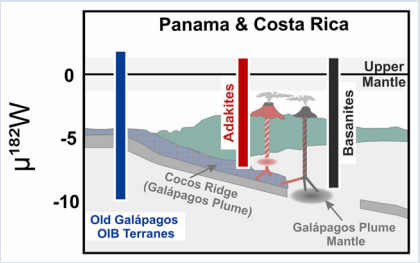

Tungsten isotope anomalies in modern rocks are exclusively associated with plume-related basalts and may provide a unique tool to identify recycled plume material in subduction zone magmatism. In Central America, the Cocos and Coiba Ridges are subducting with the Cocos plate. These ridges may introduce material into the arc magma source that was derived from the Galápagos plume, which has been shown to carry anomalous ^{182}W signatures. Here, we report negative $\mu^{182}W$ values together with trace element data for <5 Ma old adakites and back-arc basanites, as well as accreted basalt terranes that formed as a result of Galápagos plume activity in the last 70 Myr. In adakites and basanites, these $\mu^{182}W$ deficits derive from a slab melt component that dominates the W budget of their source. In addition, negative $\mu^{182}W$ in accreted mafic terranes attest to the longevity of the primordial W isotope signature in the Galápagos plume and the involvement of a Galápagos-related magma source in the Central American arc system over time.

Received 16 February 2023 | Accepted 6 June 2023 | Published 23 June 2023

Introduction

Mass transfer from variable components of the subducting oceanic lithosphere into the arc mantle and subsequent incorporation into arc magmas represents a major paradigm in Earth Sciences. While there is strong evidence for the involvement of fluids and subducted sediments in the mantle source of many arc magmas (Tera *et al.*, 1986), the nature of direct contributions of subducted basaltic crust remains debated. However, slab melting under certain conditions has become central to many models of subduction zone processes (*e.g.*, Yogodzinski *et al.*, 2015). Here, we use isotope and concentration data for W in arc-related rocks to trace slab- and plume-derived source components in arc magmas. Variations in the distribution of ^{182}W in terrestrial rocks must have been established within the first 50 Myr of Earth's history due to the short half-life of its extinct parent isotope ^{182}Hf (*e.g.*, Willbold *et al.*, 2011). The only known modern setting exhibiting negative ^{182}W variability is ocean islands associated with deep-seated mantle plumes, such as Galápagos (*e.g.*, Mundl-Petermeier *et al.*, 2020). In this context, the Central American arc system is a prime location for using W isotopes as a tracer for oceanic crust and plume-mantle components in arc magmas. Here, the 13 to 15 Ma old Cocos and Coiba Ridge (CCR), and other hotspot traces related to the Galápagos plume, are being subducted along the Panama–Costa Rica section of the Central American arc system (Hauff *et al.*, 2000; Abratis and Wörner, 2001; Gazel *et al.*, 2009, 2011). About 1.5 to 5 Ma old adakitic lavas from Panama and Costa Rica are of particular interest, since involvement of a slab melt component in their petrogenesis has previously been proposed (*e.g.*, Defant *et al.*, 1991; Abratis and Wörner, 2001; Gazel *et al.*, 2009). Identification of negative W isotope anomalies in these adakites would thus provide a strong, first-hand indication for the involvement of plume-derived subducted oceanic crust in arc melts from the Central American arc system. Further, a suite of alkaline mafic lavas (basanites) in the back-arc in Costa Rica dated at 4 to 6 Ma possibly record a mantle contribution from the Galápagos plume (Abratis and Wörner, 2001). Here, radiogenic W isotope systematics provide a powerful tracer to identify different source components that may be derived from the Galápagos plume.

Samples and Methods

We selected 14 well-characterised adakites from the Costa Rica and Panama arc front and five basanites from behind the volcanic arc of southern Costa Rica for W isotope and trace element analysis. To constrain the isotopic composition of subducted material we also analysed ocean island basalt (OIB) terranes that were accreted to the forearc of Costa Rica and Panama. The latter were interpreted to represent 18 to 71 Ma old hotspot tracks of the Galápagos plume (*e.g.*, Appel *et al.*, 1994; Hauff *et al.*, 2000; Wegner *et al.*, 2011; Gazel *et al.*, 2018). Further details on the samples as well as Sr, Pb and Nd isotope compositions can be found in Appel *et al.* (1994), Abratis and Wörner (2001) and Wegner *et al.* (2011). The W isotopic compositions are reported as $\mu^{182}W$, representing the part per million deviation of the $^{182}W/^{184}W$ ratio of a sample from W standard NIST 3163. Detailed descriptions of methods and analytical results are provided in the Supplementary Information.

1. Geoscience Center, Georg-August-Universität Göttingen, Goldschmidtstraße 1-3, 37077, Göttingen, Germany
* Corresponding author (email: nils.messling@uni-goettingen.de)

Results and Discussion

The adakites range in SiO_2 content between 53 to 69 wt. % and show high Sr/Y ratios from 100 to 200 at low Y concentrations of 7 to 14 µg/g. They feature prominent depletions in high field strength elements (HFSE) and are low in heavy rare earth elements (HREE) due to melting of hydrous meta-basalt with residual rutile and garnet (Figure S-1; Martin *et al.*, 2005). Their W isotopic compositions range from $\mu^{182}W = -6.89 \pm 2.95$ to $+0.87 \pm 2.95$ (external reproducibility, 2 s.d.). There are no observable correlations between $\mu^{182}W$ and either major or trace element concentrations, their ratios or with any radiogenic isotope ratios. Basanites have SiO_2 concentrations from 43 to 47 wt. % with high MgO of 6.3 to 9.3 wt. %. They show trace element patterns that are strongly enriched in incompatible elements with notable depletions in HFSE comparable to the adakites. Although their Sr/Y ratios are elevated compared to normal arc lava and range between 42 and 120, they also have high Y concentrations (17.5 to 30 µg/g) and are silica-undersaturated, which places them outside the compositional range expected for adakitic rocks (Martin *et al.*, 2005). Values for $\mu^{182}W$ range from -9.04 ± 4.32 to $+1.74 \pm 4.32$. Similar to the adakites, no correlations with other chemical or radiogenic isotope tracers can be observed. Accreted OIB have MgO concentrations ranging from 6 to 21 wt. %. Trace element patterns show typical intraplate affinities, similar to the modern Galápagos archipelago with enriched incompatible elements and a relative depletion in Pb. Their $\mu^{182}W$ ranges from -9.72 ± 4.8 to $+0.98 \pm 2.95$. Thus, as a first-order observation, all three rock types related to the Costa Rica–Panama subduction zone show resolvable W isotope deficits. In the following, we will address likely scenarios that can reconcile this observation.

Previous results for modern basalts from the Galápagos archipelago, together with our own data for the accreted OIB terranes, provide an approximation of the isotopic composition of the basalts from the CCR, that are currently subducted below Central America. A chemical and isotopic zonation within the Galápagos plume (Hoernle *et al.*, 2000) is mirrored by contrasting negative W isotopic compositions of basalts from the central and eastern domains of the Galápagos islands ($\mu^{182}W = -22$ and -5, respectively; Mundl-Petermeier *et al.*, 2020). This chemical zonation is also reflected in the CCR, as well as in the basaltic rocks accreted in the Central American forearc (Gazel *et al.*, 2018 and references therein). We find that the W isotopic compositions of the accreted CCR rocks analysed here do not fully reflect the entire range observed in the modern Galápagos archipelago. However, $\mu^{182}W$ deficits of up to -9.72 ± 4.80 confirm that the Galápagos plume is isotopically variable and, more importantly, show that the incorporated primordial W isotopic signature has existed for at least the past 70 Myr. This implies that the unusual W isotopic signature is a long-lived, persistent characteristic of the plume. If equivalents of such basaltic rocks from the CCR are also subducted to the depth where magmas are formed, these arc magmas would also be expected to show similar $\mu^{182}W$ deficits.

This is, in fact, supported by our observations: the $\mu^{182}W$ deficits of up to -6.89 ± 2.95 in the adakites cover almost the entire range of $\mu^{182}W$ variations measured in the accreted CCR basalts, providing a clear indication for involvement of a Galápagos plume component in their source. We will now test whether partial melts of the subducted basalts from the CCR contributed to the $\mu^{182}W$ deficits or, alternatively, the mantle wedge below Costa Rica and Panama contained material from the Galápagos plume, as was proposed for the origin of the basanites (Abratis and Wörner, 2001). The geochemical behaviour of W in subduction zones is best studied using W/Th ratios (König *et al.*, 2008). Bulk partition coefficients of W and Th are very similar during mantle melting (Arevalo and McDonough, 2008), resulting in only small variations of W/Th ratios in oceanic basalts (MORB = 0.09 to 0.24, OIB = 0.08 to 0.19; König *et al.*, 2011; Kurzweil *et al.*, 2019). During differentiation of mafic magmas, this ratio should remain constant. However, W is mobile in subduction zone fluids (Bali *et al.*, 2012), resulting in elevated W/Th ratios in arc magmas compared to MORB and OIB (Fig. 1; König *et al.*, 2008; Stubbs *et al.*, 2022). Indeed, W/Th ratios for "normal" arc lavas from Central America, with W/Th ranging from 0.05 to 0.43, fall into the global arc magma range (Fig. 1). In contrast, adakites and basanites show surprisingly low W/Th ratios between 0.02 and 0.06, substantially lower than MORB, OIB and most arc front lava previously measured. Only five of the 19 adakites and basanite samples have elevated W/Th (>0.09). These also record high Ba/Th ratios of >280 or high $^{87}Sr/^{86}Sr$ ratios of >0.704, in line with additional fluid or sedimentary components in their source (Fig. 1, Table S-1; Stubbs *et al.*, 2022). Neither involvement of slab fluids, nor the addition of an enriched mantle source, can explain the exceptionally low average W/Th ratios in the remaining adakites and basanites, because such components would result in higher, not lower, W/Th ratios. On the other hand, such low W/Th ratios could be due to melting of subducted basalts with residual rutile, where rutile preferentially retains W and other HFSE (Rudnick *et al.*, 2000; Zack *et al.*, 2002; Bali *et al.*, 2012). Strong depletions of Nb, Ta and Ti in adakites and basanites also make a strong case for the involvement of rutile (Fig. S-1). Moreover, elevated Nb/Ta ratios in both adakites (18.01 ± 1.86) and basanites (20.1 ± 1.85) compared to typical values found in oceanic basalts (Nb/Ta = 14.5 to 16.5; Gale *et al.*, 2013; Tang *et al.*, 2019) are complementary to low Nb/Ta ratios in rutile (Green and Pearson, 1987). Combined, the unusual W isotope deficits and low W/Th ratios make a strong case that the petrogenesis of adakites and basanites is linked to partial melting of a subducted metabasaltic source derived from the Galápagos plume. This either involves the slab melt directly or a mantle source modified by slab melts derived from CCR basalts.

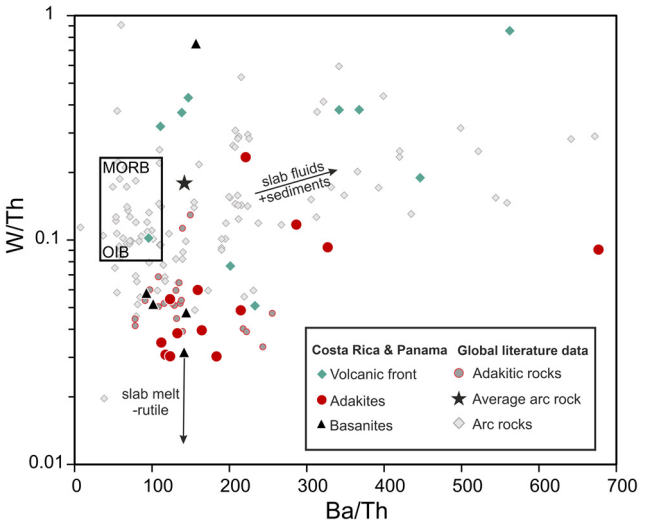

Figure 1 Fluid mobile element systematics for Panama and Costa Rica arc rocks and compiled arc data from König *et al.* (2011), Kurzweil *et al.* (2019), Mazza *et al.* (2020), and Stubbs *et al.* (2022). MORB and OIB fields defined after König *et al.* (2011) and Kurzweil *et al.* (2019). Adakitic rocks from Laeger *et al.* (2013) and Straub *et al.* (2015).

Based on the large range of silica content, it was argued that the adakites in Costa Rica and Panama do not represent pure slab melts, but rather derive from a mantle wedge metasomatised by slab melts (Gazel *et al.*, 2009, 2011; Martin *et al.*, 2005). To test this model with our data, we performed simple mixing calculations between a slab-derived melt and a subduction-modified mantle wedge (Fig. 2; see Supplementary Information for model parameters). The source of adakites is best represented by a mantle wedge metasomatised by 3 to 20 wt. % of a slab melt with low W/Th of 0.018. This is in good agreement with previous models using radiogenic isotopes (Gazel *et al.*, 2009). The variability of $\mu^{182}W$ in the adakites and the lack of correlation with other geochemical parameters require that the slab was heterogeneous in $\mu^{182}W$. Therefore, this model constrains the maximum W isotope deficit of a slab melt necessary to explain the range observed in the adakites. As shown in Figure 3a, assuming $\mu^{182}W$ values varying between −12 to 0 for the subducted CCR basalts can reconcile the isotopic compositions of most adakites. Three samples with high Ba/Th and W/Th, however, plot outside of this plausible mixing field, which is likely due to an additional component in their source.

To account for the enriched trace element signature observed in the basanites, we included an enriched source model component in our calculations. Following slab window formation below Costa Rica and Panama, previous models have argued for the ascent and decompression melting of a mantle component that was derived from the Galápagos plume as the source for the basanites (Abratis and Wörner, 2001; Gazel *et al.*, 2011). However, similar to the case of the adakites, the low W/Th ratios of the basanites require an additional slab melt component. In our model, the enriched mantle composition was estimated from the average Galápagos basalt. Melting of this enriched mantle modified by 2 to 10 wt. % slab melt formed from CCR basalts can explain the observed incompatible element enrichment in basanites while maintaining their low W/Th ratios (Figs. 2, S-2). Finally, we can test how this enriched Galápagos mantle influences the W isotopic composition of the basanites. Model A in Figure 3b uses the enriched mantle composition assuming $\mu^{182}W = 0$, while model B involves a Galápagos mantle with $\mu^{182}W$ as low as −6. Each model encompasses the observed

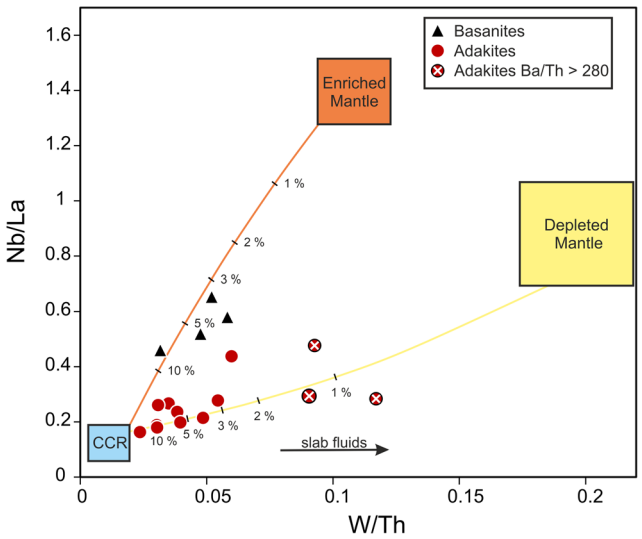

Figure 2 Two component mixing models for melts derived from a depleted mantle or an enriched mantle modified by Cocos and Coiba Ridge (CCR) melts. Endmember compositions and model parameters can be found in the Supplementary Information. Samples with W/Th > 0.2 not shown.

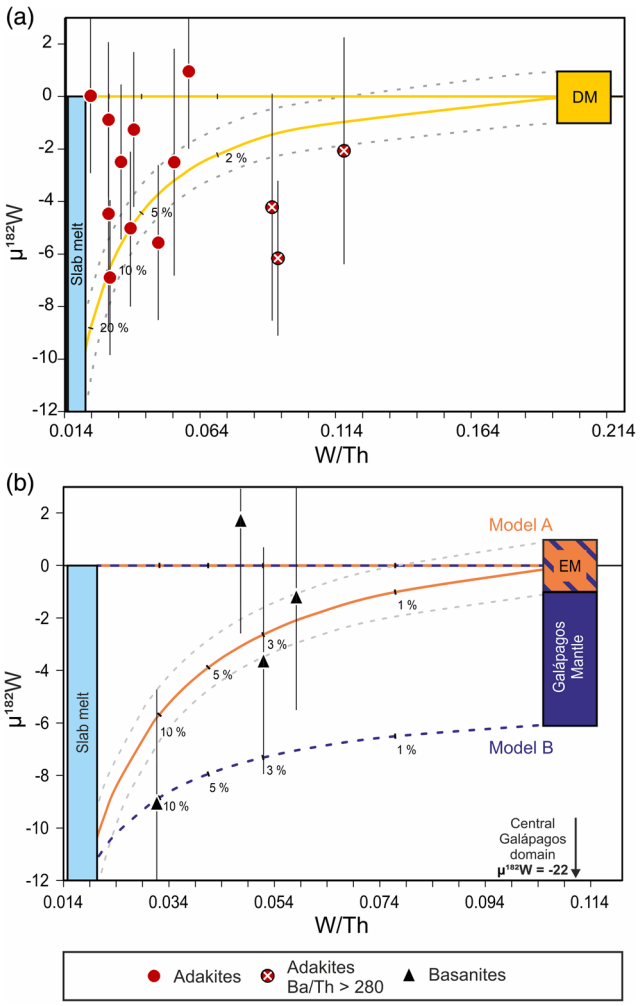

Figure 3 Two component mixing models between modelled slab melt and three different mantle compositions: **(a)** mixing with depleted mantle to model the W isotope composition of adakites and **(b)** mixing with two types of enriched mantle (models A and B) to produce the source composition of basanites. Grey dashed lines represent the error of the W isotopic composition of the upper mantle. Model parameters can be found in the Supplementary Information.

basanite compositions including the most anomalous basanite ($\mu^{182}W = -9.04 \pm 4.32$). Model A, however, shows that contributions of isotopically anomalous W from the enriched mantle source are not required to explain the variability observed in the basanites. If this mantle source is characterised by depletions in $\mu^{182}W$, values cannot be significantly lower than −6, as it is shown in model B. It is therefore unlikely that this component reflects the composition of the modern central Galápagos domain (Bekaert *et al.*, 2021). In any case, the negative W isotope signal observed in adakties and basanites from Costa Rica and Panama requires a slab melt component that carries the anomalous $\mu^{182}W$ from the Galápagos plume.

Conclusions

The tungsten isotope systematics of the adakites verify melting of subducted oceanic crust at mantle depth in the Central American arc system. Melts derived from a hybridised mantle wedge with negative $\mu^{182}W$ signatures provide strong evidence that this contribution is related to Cocos and Coiba Ridges

(CCR). In the case of the back-arc basanites, this signature is possibly modified by mantle components derived from the Galápagos plume, although their contribution is not strictly required to explain their isotopic budget. Unusually low W/Th in both adakites and basanites imply control by residual rutile on the W budget of their sources. These observations further strengthen previous proposals for magma genesis for these adakites and basanites related to the evolution of a slab window below Costa Rica and Panama as a consequence of CCR collision with the Central American subduction zone. Finally, we document that the anomalous low $\mu^{182}W$ signal is a long-lived (>70 Myr) geochemical signature of the Galápagos plume.

Acknowledgements

This study was funded through the Priority Programme 1833 "Building a Habitable Earth" of the German Science Foundation (DFG grant No. WI 3579/3-1 to MW). GW acknowledges DFG grants No. WO 362/10 and WO 362/27-2 for providing funds for sampling in the field. We thank Caroline Soderman and Jonas Tusch for their constructive review of the manuscript and Helen Williams for editorial handling. M. Abratis, W. Wegner, S. Rausch, and R. Harmon are thanked for their efforts during strenuous fieldwork in Central America. We acknowledge Rachel Bezard for helpful discussions and Dirk Hoffmann for support with mass spectrometry and clean lab maintenance.

Editor: Helen Williams

Additional Information

Supplementary Information accompanies this letter at https://www.geochemicalperspectivesletters.org/article2321.

Cite this letter as: Messling, N., Wörner, G., Willbold, M. (2023) Ancient mantle plume components constrained by tungsten isotope variability in arc lavas. *Geochem. Persp. Let.* 26, 31–35. https://doi.org/10.7185/geochemlet.2321

References

Abratis, M., Wörner, G. (2001) Ridge collision, slab-window formation, and the flux of Pacific asthenosphere into the Caribbean realm. *Geology* 29, 127–130. https://doi.org/10.1130/0091-7613(2001)029<0127:RCSWFA>2.0.CO;2

Appel, H., Wörner, G., Alvarado, G., Rundle, C., Kussmaul, S. (1994) Age relations in igneous rocks from Costa Rica. *Profil* 7, 63–69.

Arevalo Jr., R., McDonough, W.F. (2008) Tungsten geochemistry and implications for understanding the Earth's interior. *Earth and Planetary Science Letters* 272, 656–665. https://doi.org/10.1016/j.epsl.2008.05.031

Bali, E., Keppler, H., Audetat, A. (2012) The mobility of W and Mo in subduction zone fluids and the Mo–W–Th–U systematics of island arc magmas. *Earth and Planetary Science Letters* 351–352, 195–207. https://doi.org/10.1016/j.epsl.2012.07.032

Bekaert, D.V., Gazel, E., Turner, S., Behn, M.D., de Moor, J.M., *et al.* (2021) High $^{3}He/^{4}He$ in central Panama reveals a distal connection to the Galápagos plume. *Proceedings of the National Academy of Sciences* 118, e2110997118. https://doi.org/10.1073/pnas.2110997118

Defant, M.J., Clark, L.F., Stewart, R.H., Drummond, M.S., de Boer, J.Z., Maury, R.C., Bellon, H., Jackson, T.E., Restrepo, J.F. (1991) Andesite and dacite genesis via contrasting processes: the geology and geochemistry of El Valle Volcano, Panama. *Contributions to Mineralogy and Petrology* 106, 309–324. https://doi.org/10.1007/BF00324560

Gale, A., Dalton, C.A., Langmuir, C.H., Su, Y., Schilling, J.-G. (2013) The mean composition of ocean ridge basalts. *Geochemistry, Geophysics, Geosystems* 14, 489–518. https://doi.org/10.1029/2012GC004334

Gazel, E., Carr, M.J., Hoernle, K., Feigenson, M.D., Szymanski, D., Hauff, F., van de Bogaard, P. (2009) Galapagos-OIB signature in southern Central America: Mantle refertilization by arc–hot spot interaction. *Geochemistry, Geophysics, Geosystems* 10, Q02S11. https://doi.org/10.1029/2008GC002246

Gazel, E., Hoernle, K., Carr, M.J., Herzberg, C., Saginor, I., van den Bogaard, P., Hauff, F., Feigenson, M., Swisher III, C. (2011) Plume–subduction interaction in southern Central America: Mantle upwelling and slab melting. *Lithos* 121, 117–134. https://doi.org/10.1016/j.lithos.2010.10.008

Gazel, E., Trela, J., Bizimis, M., Sobolev, A., Batanova, V., Class, C., Jicha, B. (2018) Long-Lived Source Heterogeneities in the Galapagos Mantle Plume. *Geochemistry, Geophysics, Geosystems* 19, 2764–2779. https://doi.org/10.1029/2017GC007338

Green, T.H., Pearson, N.J. (1987) An experimental study of Nb and Ta partitioning between Ti-rich minerals and silicate liquids at high pressure and temperature. *Geochimica et Cosmochimica Acta* 51, 55–62. https://doi.org/10.1016/0016-7037(87)90006-8

Hauff, F., Hoernle, K., van den Bogaard, P., Alvarado, G., Garbe-Schönberg, D. (2000) Age and geochemistry of basaltic complexes in western Costa Rica: Contributions to the geotectonic evolution of Central America. *Geochemistry, Geophysics, Geosystems* 1, 1009. https://doi.org/10.1029/1999GC000020

Hoernle, K., Werner, R., Morgan, J.P., Garbe-Schönberg, D., Bryce, J., Mrazek, J. (2000) Existence of complex spatial zonation in the Galápagos plume. *Geology* 28, 435–438. https://doi.org/10.1130/0091-7613(2000)28<435:EOCSZI>2.0.CO;2

König, S., Münker, C., Schuth, S., Garbe-Schönberg, D. (2008) Mobility of tungsten in subduction zones. *Earth and Planetary Science Letters* 274, 82–92. https://doi.org/10.1016/j.epsl.2008.07.002

König, S., Münker, C., Hohl, S., Paulick, H., Barth, A.R., Lagos, M., Pfänder, J., Büchl, A. (2011) The Earth's tungsten budget during mantle melting and crust formation. *Geochimica et Cosmochimica Acta* 75, 2119–2136. https://doi.org/10.1016/j.gca.2011.01.031

Kurzweil, F., Münker, C., Grupp, M., Braukmüller, N., Fechtner, L., Christian, M., Hohl, S.V., Schoenberg, R. (2019) The stable tungsten isotope composition of modern igneous reservoirs. *Geochimica et Cosmochimica Acta* 251, 176–191. https://doi.org/10.1016/j.gca.2019.02.025

Laeger, K., Halama, R., Hansteen, T., Savov, I.P., Murcia, H.F., Cortés, G.P., Garbe-Schönberg, D. (2013) Crystallization conditions and petrogenesis of the lava dome from the ~900 years BP eruption of Cerro Machín Volcano, Colombia. *Journal of South American Earth Sciences* 48, 193–208. https://doi.org/10.1016/j.jsames.2013.09.009

Martin, H., Smithies, R.H., Rapp, R., Moyen, J.-F., Champion, D. (2005) An overview of adakite, tonalite–trondhjemite–granodiorite (TTG), and sanukitoid: relationships and some implications for crustal evolution. *Lithos* 79, 1–24. https://doi.org/10.1016/j.lithos.2004.04.048

Mazza, S.E., Stracke, A., Gill, J.B., Kimura, J.-I., Kleine, T. (2020) Tracing dehydration and melting of the subducted slab with tungsten isotopes in arc lavas. *Earth and Planetary Science Letters* 530, 115942. https://doi.org/10.1016/j.epsl.2019.115942

Mundl-Petermeier, A., Walker, R.J., Fischer, R.A., Lekic, V., Jackson, M.G., Kurz, M.D. (2020) Anomalous ^{182}W in high $^{3}He/^{4}He$ ocean island basalts: Fingerprints of Earth's core? *Geochimica et Cosmochimica Acta* 271, 194–211. https://doi.org/10.1016/j.gca.2019.12.020

Rudnick, R.L., Barth, M., Horn, I., McDonough, W.F. (2000) Rutile-Bearing Refractory Eclogites: Missing Link Between Continents and Depleted Mantle. *Science* 287, 278–281. https://doi.org/10.1126/science.287.5451.278

Straub, S.M., Gómez-Tuena, A., Bindeman, I.N., Bolge, L.L., Brandl, P.A., *et al.* (2015) Crustal recycling by subduction erosion in the central Mexican Volcanic Belt. *Geochimica et Cosmochimica Acta* 166, 29–52. https://doi.org/10.1016/j.gca.2015.06.001

Stubbs, D., Yang, R., Coath, C.D., John, T., Elliott, T. (2022) Tungsten isotopic fractionation at the Mariana arc and constraints on the redox conditions of subduction zone fluids. *Geochimica et Cosmochimica Acta* 334, 135–154. https://doi.org/10.1016/j.gca.2022.08.005

Tang, M., Lee, C.-T.A., Chen, K., Erdman, M., Costin, G., Jiang, H. (2019) Nb/Ta systematics in arc magma differentiation and the role of arclogites in continent formation. *Nature Communications* 10, 235. https://doi.org/10.1038/s41467-018-08198-3

Tera, F., Brown, L., Morris, J., Sacks, I.S., Klein, J., Middleton, R. (1986) Sediment incorporation in island-arc magmas: Inferences from ^{10}Be. *Geochimica et Cosmochimica Acta* 50, 535–550. https://doi.org/10.1016/0016-7037(86)90103-1

Wegner, W., Wörner, G., Harmon, R.S., Jicha, B.R. (2011) Magmatic history and evolution of the Central American Land Bridge in Panama since Cretaceous times. *Bulletin of the Geological Society of America* 123, 703–724. https://doi.org/10.1130/B30109.1

Willbold, M., Elliott, T., Moorbath, S. (2011) The tungsten isotopic composition of the Earth's mantle before the terminal bombardment. *Nature* 477, 195–198. https://doi.org/10.1038/nature10399

Yogodzinski, G.M., Brown, S.T., Kelemen, P.B., Vervoort, J.D., Portnyagin, M., Sims, K.W.W., Hoernle, K., Jicha, B.R., Werner, R. (2015) The Role of Subducted Basalt in the Source of Island Arc Magmas: Evidence from Seafloor Lavas of the Western Aleutians. *Journal of Petrology* 56, 441–492. https://doi.org/10.1093/petrology/egv006

Zack, T., Kronz, A., Foley, S.F., Rivers, T. (2002) Trace element abundances in rutiles from eclogites and associated garnet mica schists. *Chemical Geology* 184, 97–122. https://doi.org/10.1016/S0009-2541(01)00357-6

Geochemical Perspectives Letters

Ancient mantle plume components constrained by tungsten isotope variability in arc lavas

N. Messling, G. Wörner, M. Willbold

Supplementary Information

The Supplementary Information includes:

- Methods
- Binary Mixing Models
- Supplementary Tables S-1 to S-5
- Supplementary Figures S-1 to S-5
- Supplementary Information References

Methods

Analytical techniques utilised in this study are based on W separation procedures described in earlier work (Willbold *et al.*, 2011; Mei *et al.*, 2018; Tusch *et al.*, 2019). We further optimised the W separation procedure for larger sample sizes while maintaining measurement precision and accuracy. Therefore, we devised a new W separation procedure to process up to 6 g of sample material on a three-step ion exchange chromatography. We utilised the precipitation of a W-free fluoride phase during sample digestion, which removed the majority of matrix elements, while quantitatively retaining W. Sample preparation was carried out under metal-free clean laboratory conditions at the University of Göttingen.

1. Sample preparation and trace element measurement

All adakites and basanites were available as powders that were initially used by Abratis and Wörner (2001) and Wegner *et al.* (2011). These powders were prepared using an agate ball mill after crushing in the field and washing with distilled water. Additional samples from accreted fore-arc terranes (QUE-020, PAR-023 and PAV-030) were crushed into 1–2 cm large chips in a steel jaw crusher. To avoid metal contamination the samples were then washed with Milli-Q water (Merck Millipore). After drying, the chips were packed into plastic bags and crushed with a hydraulic press into pieces smaller than 5 mm. The crushed samples were ground in agate ball mills and used for trace element and isotopic analysis. The new trace element measurements were conducted as described in Hegner *et al*. (2022) on a ThermoFisher Scientific iCap Q-ICPMS. Sample powders were digested in a picotrace DAS high-pressure digestion system at 220 °C in 1.2 mL concentrated HF and 0.3 mL concentrated HNO_3 to ensure complete digestion of refractory minerals. In addition, reference materials ranging from basalts to rhyolites were equally prepared in order to accurately represent the compositional range of samples measured in this study.

2. Tungsten sample digestion and separation

All steps were carried out using double distilled acids (Savillex DST-1000) or ultra-pure reagents, which were diluted to appropriate concentrations using 18.2 MΩ cm water (Merck Millipore Milli-Q). Between 2 and 6 g of sample powder were weighed out in 60 or 90 mL Savillex beakers. For every 2 g of sample powder, 10 mL 6 M HCl and 10 mL 24 M HF were added. In the closed beaker the samples were digested at 150 °C for 3 days, ultrasonicating the samples at the beginning and end of the digestion. After completely drying down the sample at 130 °C, 10 mL 0.5 M HCl–1 M HF were added and heated for 1–2 h. The samples were transferred into a 50 mL centrifuge tube and centrifuged for 15 min. The acid supernatant was decanted and stored in another centrifuge tube. To the fluoride residue, another 10 mL 0.5 M HCl–1 M HF were added, which was then placed into a heated ultrasonic bath at 60 °C for 15 min. After centrifuging and decanting this step was repeated once more. W was quantitively transferred into the supernatant at this point (Fig. S-3a). The fluoride residue, containing a significant fraction of matrix elements was therefore discarded. The 30 mL of the combined supernatant were used for the ion exchange procedure. The full elution scheme of all ion exchange procedures used is described in Table S-2. After the first anion (10 mL AG1x8) chemistry the sample solution was directly passed through an Eichrom prefilter column to remove dissolved organic compounds. After this step and every following ion exchange chromatography samples were treated with HNO_3–H_2O_2 as described in Tusch *et al.* (2019). On the following 1 mL TEVA column, W was separated from the remaining HFSE as described in Mei *et al.* (2018). Lastly, a 1 mL anion clean-up chemistry was used to separate remaining matrix elements. For several samples, an aliquot was taken after the digestion of the samples to show no W is lost during the fluoride precipitation procedure. Typically, 60–90 % of the W budget of the samples is recovered using this chemical separation procedure (Fig. S-3b). Further, we compared digestion yields of the reference material JB-2 for complete digestion and fluoride precipitation digestion. All results are provided in Figure S-3a. Procedural blanks for the entire chemical separation procedure ranged from 96 to 841 pg for every 6 g of digested material, with an average of 346 pg (n = 9) corresponding to an average blank contribution of 0.6 ‰. Elution patterns for the first anion and the TEVA exchange chromatography for some matrix elements and the HFSE is provided in Figure S-4.

3. Tungsten isotope measurement

The W isotopic compositions of samples and reference materials were determined on a Thermo Fisher Scientific Neptune Plus MC-ICP-MS at the University of Göttingen. A Teledyne Cetac Aridus III desolvating nebuliser equipped with the Teledyne Cetac QuickWash3 accessory was used as the sample introduction system. Similar to Tusch *et al.* (2019), a cyclonic quartz spray chamber was interconnected between the desolvating nebuliser and the torch to improve the signal stability by increasing the expansion volume of the inlet system. Faraday cups were connected to a series of 10^{11}, 10^{12} and 10^{13} Ω amplifier boards to measure ion currents of the W isotopes, as well as those of ^{177}Hf, ^{178}Hf, ^{181}Ta and ^{188}Os, which were monitored for the correction of isobaric interferences on W. 10^{11} Ω amplifiers were used for ^{177}Hf, ^{182}W, ^{183}W, ^{184}W and ^{186}W, whereas ^{188}Os was monitored using a 10^{12} Ω amplifier and ^{178}Hf and ^{180}W using a 10^{13} Ω amplifier. Typical sensitivities with a Ni standard sample cone and X skimmer cone and a 60 µL/min nebuliser were 300–350 V/ppm of total W. Triplet analyses were conducted for each sample, with 60 cycles and an integration time of 8.39 seconds per analysis. For samples with high W concentrations 6 individual measurements were conducted. Each sample was bracketed with a 240 ng/g W NIST SRM 3163 solution. Data reduction was carried out offline using a Python script using exponential law to correct for mass bias, normalising to $^{186}W/^{184}W$ = 0.92767 (Völkening *et al.*, 1991). For a high-precision triplet measurement, ~650 ng of W were required. The external reproducibility was calculated by repeated measurements of in-house reference materials ‘Granite 232’ (described in Haack, 1969) and ‘Basalt Me21’, collected from the ‘Hoher Meißner’ basalt quarry, that were measured at the beginning and the end of every measurement sequence (Fig. S-5). Data is expressed as $\mu^{182}W$ which is defined as $(^{182}W/^{184}W_{sample} / {}^{182}W/^{184}W_{NIST\ 3163} - 1) \times 1{,}000{,}000$. The external $\mu^{182}W$

reproducibility (2 s.d.) for Granite 232 is 3.61 ppm (n = 13) and 4.36 ppm for Me21 (n = 24) for triplet measurements. For sextuplet analysis, the reproducibility was improved to 2.95 ppm for Me21 (n = 8), in good agreement with the external reproducibility reported in recent literature (2.9–4.5 ppm, Jansen *et al.*, 2022; 1.45–2.73 ppm, Tusch *et al.*, 2022). The W isotope data for single measurements is provided in Figure S-4 together with $\mu^{183}W$ data and values normalised to $^{186}W/^{183}W$. This also includes $\mu^{182}W$ values (normalised to $^{186}W/^{183}W$), corrected for mass-independent fractionation with the equation from Budde *et al.* (2022). We observe mass-independent W isotope variations resulting in deficits in $\mu^{182}W$ as low as -20 ppm, similar to previous studies (Kruijer and Kleine, 2018; Archer *et al.*, 2019; Tusch *et al.*, 2019; Tappe *et al.*, 2020; Budde *et al.*, 2022). This effect likely occurs during the dry-down procedure between ion exchange chromatography steps and often coincides with significant losses of W (Willbold *et al.*, 2011; Tusch *et al.*, 2019; Budde *et al.*, 2022). We applied the dry-down procedure described by Tusch *et al.* (2019), adding several steps of HNO_3–H_2O_2 to the W cuts following the dry-down after each chromatography step. However, this procedure does not result in a decrease in the ^{183}W effect in our samples. The precipitation of fluorides likely has no influence on the analytical ^{183}W effect, since the magnitude of this effect is in line with previous methods that applied a complete digestion procedure (Tusch *et al.*, 2019). In this study, we used $^{186}W/^{184}W$ for the mass bias correction to avoid any analytical effects of ^{183}W. When corrected for mass-independent fractionation (Budde *et al.*, 2022), $\mu^{182}W$ values normalised to $^{186}W/^{183}W$ are in good agreement with those normalised to $^{186}W/^{184}W$ within 3 ppm (Table S-4).

Binary Mixing Models

The models shown in Figures 2 and 3 are based on simple binary mixing calculations between a mantle wedge with a depleted mantle or enriched mantle composition. All parameters relevant for modelling are summarised in Table S-3. In the model, we assume a slab melt composition that was produced by partially melting a protolith with a composition of the average CCR basalts and a residual eclogitic mineral assemblage from Gazel *et al.* (2009). We calculated the HFSE abundances in the slab melt using partition coefficients from Kessel *et al.* (2005). We did not use Nb/La ratios reported in Gazel *et al.* (2009), since these were higher than the Nb/La ratios measured in the adakites. Partition coefficients for W between melt and rutile during slab melting are poorly constrained. The W/Th ratio was therefore estimated based on the lowest W/Th ratio of the adakites (W/Th = 0.023) as well as their major element chemistry (SiO_2 = 53 to 69 wt. %). For instance, assuming a slab melt W/Th ratio >0.019 would require a 35 % contribution from the slab melt, resulting in an unrealistically high SiO_2 (>57 wt. %) content in the hybridised bulk mantle composition. On the other end of the spectrum, assuming a W/Th ratio <0.014 for the slab melt, a W isotope deficit exceeding the composition of basalts from the modern central Galápagos domain ($\mu^{182}W > -22$) would be necessary to achieve the measured W isotopic composition of the adakites with this model. The currently subducting Cocos and Coiba ridges fully reflect the chemical zonation of the Galápagos Archipelago (*e.g.*, Werner *et al.*, 2003). It is therefore unlikely that the W isotopic composition of the subducted ridges only represent the central Galápagos domain. As such, we assume an intermediary W/Th ratio of 0.018 in our model, yielding slab melt contributions of 3 to 20 % that are in good agreement with radiogenic isotope modelling from Gazel *et al.* (2009). As a result, the slab melt components in the central American arc system only require a $\mu^{182}W$ isotope composition of 0 to −12. This range is in line with the isotopic composition of accreted OIB terranes measured in this study as well as basalts from the Galápagos Archipelago. The $\mu^{182}W$ value of the upper mantle is assumed to be 0 (*e.g.*, Willbold *et al.*, 2011; Jansen *et al.*, 2022). To estimate an error for this value we used the reproducibility of our standard (95 % confidence interval: $\mu^{182}W$ = 0.98) in our model calculations. Addition of sediment can potentially provide significant contributions to the W budget in arc melts. Trace element systematics in Central American arc rock generally show decreasing sediment addition towards the

southeast (Leeman *et al.*, 1994; Patino *et al.*, 2000). In southern Costa Rica and Panama, sediment contribution to arc rocks is considered small (Bekaert *et al.*, 2021). Previous models assumed a contribution of 0.1 to 0.6 % sediment-derived melts for arc rocks in this region (Gazel *et al.*, 2009). The 'global subducted sediment' (GLOSS) composite by Plank and Langmuir (1998) does not report concentration data for W. We therefore used a W/Th ratio of 0.21 based on global W sediment data (Kirchenbaur and Münker, 2015; Kurzweil *et al.*, 2019; Stubbs *et al.*, 2022) to calculate the W concentration in the sediment melt. This likely overestimates the W contribution of sediments, as residual rutile in the sediments during subduction would result in lower W/Th ratios in the melt. However, using the maximum W/Th ratios calculated here for sediment melts and the sediment proportions estimated in Gazel *et al.* (2009), the maximum contribution of sediment melt to the average W budget of adakites is less than 4 % (<13.5 ng/g). We used the lower bound of 0.1 % sediment proportion for our calculations. Based on the model of influx and arc parallel mantle flow beneath Costa Rica and Panama (Abratis and Wörner, 2001; Hoernle *et al.*, 2008) it is reasonable to assume that the mantle wedge has been modified by subduction zone processes. To account for this, we used upper mantle W concentration of 10 ng/g for the mantle source with slightly elevated W/Th ratios of 0.19 similar to the average arc basalt (König *et al.*, 2008, 2011; Mazza *et al.*, 2020; Stubbs *et al.*, 2022). The trace element budget of the enriched Galápagos mantle source was back-calculated using the average Galápagos basalt composition compiled from the GEOROC database, while assuming 11 % batch melting of the Galápagos mantle (White *et al.*, 1993). We assumed a constant W/Th of 0.11 in agreement with W/Th ratios measured in accreted Galápagos OIB terranes as well as global OIB data (König *et al.*, 2011; Kurzweil *et al.*, 2019).

Supplementary Tables

Table S-1 W isotope and long-lived radiogenic isotope data and trace element data for reanalysed samples.

Tables S-1 (.xlsx) is available for download from the online version of this article at https://doi.org/10.7185/geochemlet.2321.

Table S-2 Tungsten ion exchange matrix separation procedure.

Step	Reagent	Acid volume (mL)
I. BioRad AG1x8 100–200 mesh, 10 mL resin (20 mL Bio-Rad Econo-Pac® columns)		
Clean	1 mM DTPA–1 M HCl	4 × 10
	3 M HNO_3–0.2 M HF	4 × 10
	6 M HNO_3–0.2 M HF	4 × 10
	H_2O	4 × 10
Condition	0.5 M HCl–1 M HF	4 × 10
Load	0.5 M HCl–1 M HF	3 × 10
Elute Matrix	0.005 M HCl–1 M HF	4 × 10
Elute HFSE and Ti	0.5 M HCl–1 % H_2O_2	10 × 10
	0.005 M HCl–1 M HF	1 × 10
Collect Mo, W, Sn	3 M HNO_3–0.2 M HF	5.5 × 10

Table S-2 continued.

Step	Reagent	Acid volume (mL)
II. Eichrom prefilter resin 100–150 mesh, 1 mL resin (2 mL Biorad Poly-Prep® columns)		
Clean	3 M HCl–0.2 M HF	2 × 10
	6 M HNO_3–0.2 M HF	2 × 10
	H_2O	1 × 10
Condition	3 M HNO_3–0.2 M HF	2 × 2
Load & Collect	3 M HNO_3–0.2 M HF	55
Collect	3 M HNO_3–0.2 M HF	2 × 1
III. Eichrom TEVA 100–150 mesh, 1 mL resin (2 mL Biorad Poly-Prep® columns) on 0.4 mL Eichrom prefilter resin		
Clean	6 M HNO_3–0.2 M HF	2 × 10
	H_2O	1 × 10
	3 M HCl–0.02 M HF	2 × 10
Condition	9 M HCl–0.02 M HF	4 × 1
Load	9 M HCl–0.02 M HF	2
Rinse	9 M HCl–0.02 M HF	5 × 0.5
Collect W	3 M HCl–0.02 M HF	4 × 2
Collect Mo	3 M HNO_3–0.2 M HF	3 × 2
IV. BioRad AG1x8 100–200 mesh, 1 mL resin (2 mL Biorad Poly-Prep® columns) on 0.4 mL Eichrom prefilter resin		
Clean	0.5 M HCl–1 M HF	1 × 10
	3 M HNO_3–0.2 M HF	1 × 10
	6 M HNO_3–0.2 M HF	1 × 10
	H_2O	2 × 2
Condition	0.5 M HCl–1 M HF	4 × 1
Load	0.5 M HCl–1 M HF	3
Elute Matrix	0.005 M HCl–1 M HF	3 × 1
Collect W	3 M HNO_3–0.2 M HF	3 × 2

Table S-3 Parameters used for the binary mixing models.

Parameter	CCR slab melt	Sediment melt	Mantle wedge	Enriched mantle	Galápagos mantle
W (ng/g)	112	2250	10	14	14[e]
W/Th	0.018	0.21[c,d]	0.19	0.11[b,c]	0.11
Nb/La	0.16	0.16[a]	0.9[f]	1.3[c]	1.4[e]
$\mu^{182}W$	0 to −12	0	0	0	0 to −6

[a] Gazel *et al*. (2009).
[b] König *et al*. (2011).
[c] Kurzweil *et al*. (2019).
[d] Kirchenbaur and Münker (2015); Stubbs *et al*. (2022).
[e] Calculated from basalt data compiled from https://georoc.eu on 22 November 2022 (Geist *et al.*, 2002, 2005, 2006; Gibson and Geist, 2010; Gibson *et al.*, 2012, 2016; Handley *et al.*, 2011; Harpp and Weis, 2020; Harpp *et al.*, 2003; Peterson *et al.*, 2017, 2014).
[f] Salters and Stracke (2004).

Table S-4 W isotope data for single measurements of samples and in-house reference materials, including values normalised to $^{186}W/^{184}W$ and $^{186}W/^{183}W$.

Table S-5 Trace element concentrations of the acid supernatant from reference material JB-2 after the fluoride leaching procedure.

Tables S-4 and S-5 (.xlsx) are available for download from the online version of this article at https://doi.org/10.7185/geochemlet.2321.

Supplementary Figures

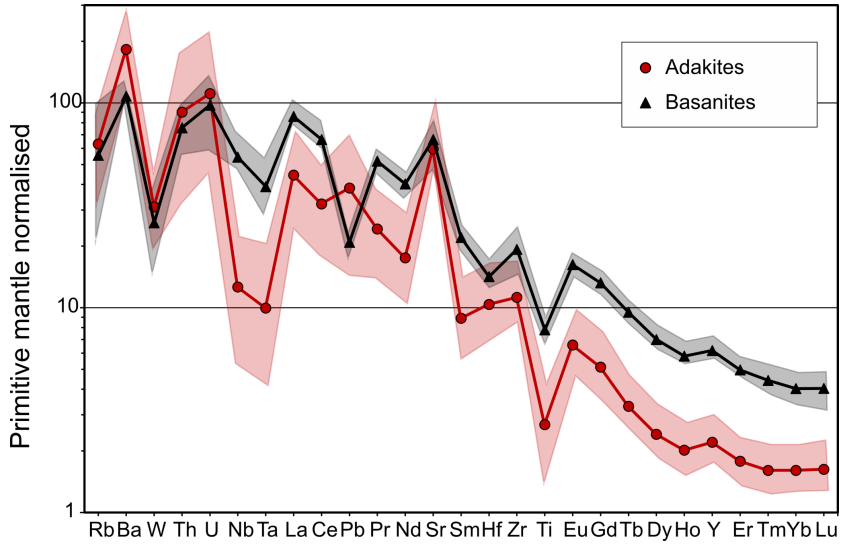

Figure S-1 Primitive mantle-normalised trace element patterns for average concentrations of adakites and basanites analysed for W isotopes. Shaded areas represent the entire trace element variability of each group. Primitive mantle values from Palme and O'Neill (2014).

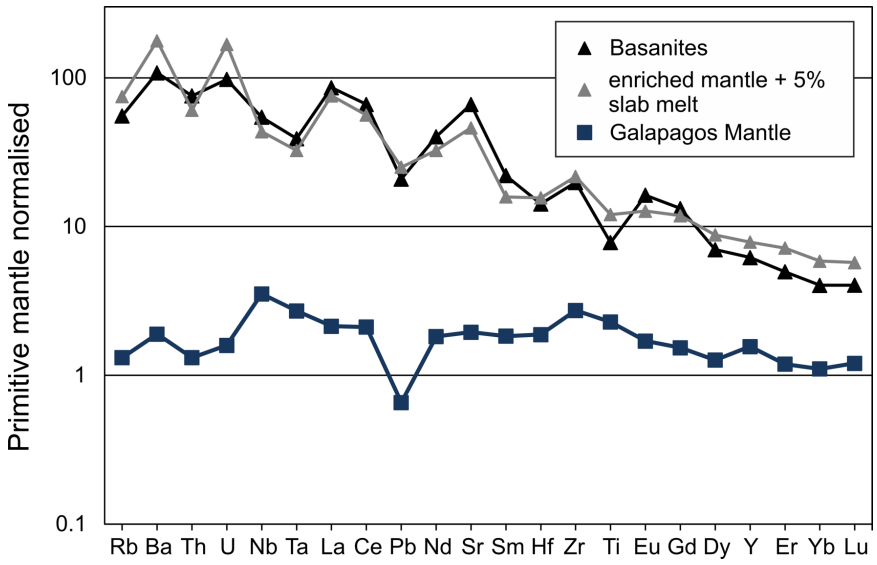

Figure S-2 Primitive mantle-normalised trace element patterns of average measured basanites plotted together with the modelled basanite melt composition. The model calculation assumes low degree melting of an enriched mantle source modified by 5 % slab melt as constrained by the modelled Nb/La and W/Th ratios shown in Figure 2. Also shown is the modelled composition of the Galápagos mantle assuming that the average Galápagos basalt was derived by 11 % batch melting of the mantle source. See text for further explanation. Primitive mantle values from Palme and O'Neill (2014).

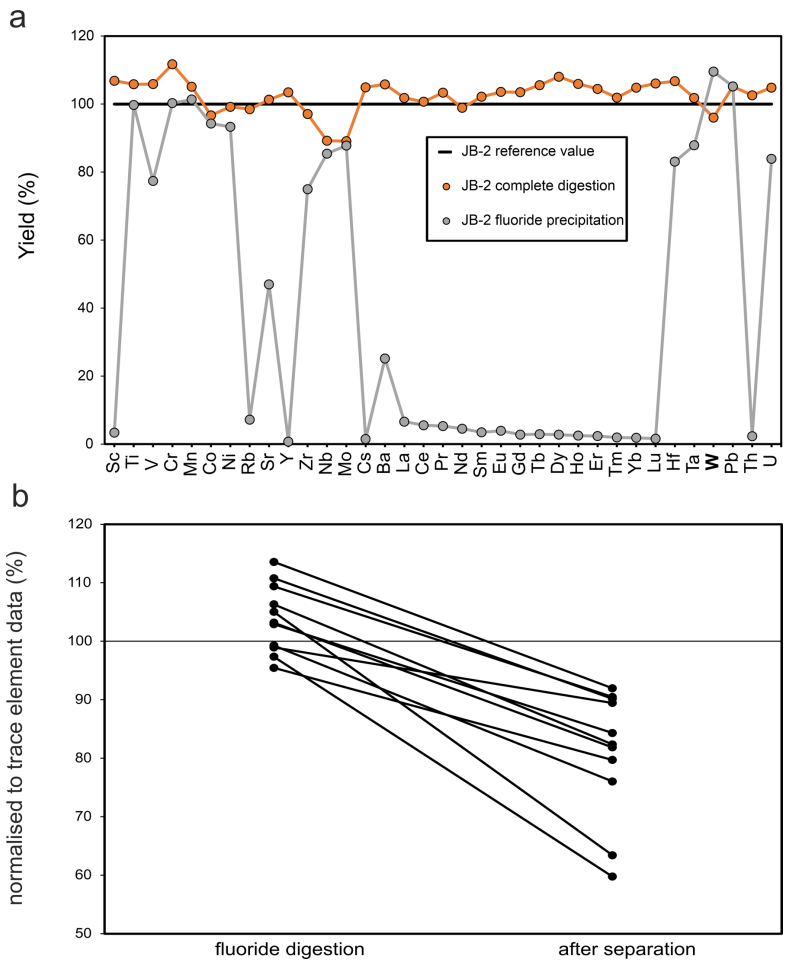

Figure S-3 **(a)** Chemistry yield of different digestion methods for selected trace elements. The fluoride-precipitation digestion was prepared under the same conditions as samples analysed for W isotopes. Normalisation values are the compiled values from for GSJ basaltic reference material JB-2 from Jochum *et al.* (2016). Trace element concentration data provided in Table S-5. **(b)** Chemistry yield from W separation procedure determined from 1 ‰ aliquots taken after sample digestion and after the separation procedure on selected samples.

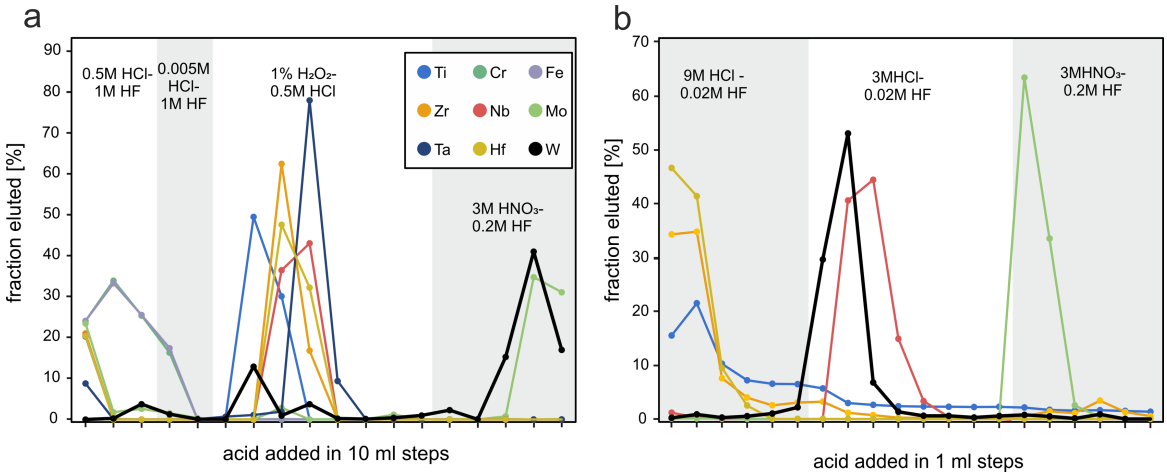

Figure S-4 Elution curves of selected elements for matrix separation procedures described in Table S-2. **(a)** I. Anion exchange chemistry (BioRad AG1x8 100–200 mesh, 10 mL resin). **(b)** III. TEVA chemistry **(**Eichrom TEVA 100–150 mesh, 1 mL resin).

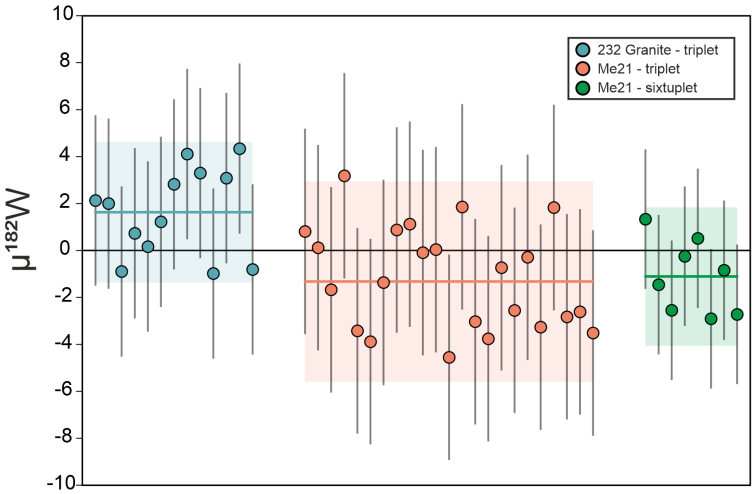

Figure S-5 $\mu^{182}W$ values of in-house reference materials Granite 232 and Me21 basalt measured over the course of two years. Coloured lines show average values of the samples. Lightly coloured areas mark the 2 s.d. calculated for each sample or method.

Supplementary Information References

Abratis, M. (1998) *Geochemical variations in magmatic rocks from southern Costa Rica as a consequence of Cocos Ridge subduction and uplift of the Cordillera de Talamanca*. PhD thesis, Universität Göttingen. http://hdl.handle.net/11858/00-1735-0000-0006-B338-3

Abratis, M., Wörner, G. (2001) Ridge collision, slab-window formation, and the flux of Pacific asthenosphere into the Caribbean realm. *Geology* 29, 127–130. https://doi.org/10.1130/0091-7613(2001)029<0127:RCSWFA>2.0.CO;2

Appel, H., Wörner, G., Alvarado, G., Rundle, C., Kussmaul, S. (1994) Age relations in igneous rocks from Costa Rica. *Profil* 7, 63–69.

Archer, G.J., Brennecka, G.A., Gleißner, P., Stracke, A., Becker, H., Kleine, T. (2019) Lack of late-accreted material as the origin of ^{182}W excesses in the Archean mantle: Evidence from the Pilbara Craton, Western Australia. *Earth and Planetary Science Letters* 528, 115841. https://doi.org/10.1016/j.epsl.2019.115841

Bekaert, D.V., Gazel, E., Turner, S., Behn, M.D., de Moor, J.M., *et al.* (2021) High ^{3}He/^{4}He in central Panama reveals a distal connection to the Galápagos plume. *Proceedings of the National Academy of Sciences* 118, e2110997118. https://doi.org/10.1073/pnas.2110997118

Budde, G., Archer, G.J., Tissot, F.L.H., Tappe, S., Kleine, T. (2022) Origin of the analytical ^{183}W effect and its implications for tungsten isotope analyses. *Journal of Analytical Atomic Spectrometry* 37, 2005–2021. https://doi.org/10.1039/D2JA00102K

Gazel, E., Carr, M.J., Hoernle, K., Feigenson, M.D., Szymanski, D., Hauff, F., van de Bogaard, P. (2009) Galapagos-OIB signature in southern Central America: Mantle refertilization by arc–hot spot interaction. *Geochemistry, Geophysics, Geosystems* 10, Q02S11. https://doi.org/10.1029/2008GC002246

Geist, D., White, W.M., Albarede, F., Harpp, K., Reynolds, R., Blichert-Toft, J., Kurz, M.D. (2002) Volcanic evolution in the Galápagos: The dissected shield of Volcan Ecuador. *Geochemistry, Geophysics, Geosystems* 3, 1061. https://doi.org/10.1029/2002GC000355

Geist, D.J., Naumann, T.R., Standish, J.J., Kurz, M.D., Harpp, K.S., White, W.M., Fornari, D.J. (2005) Wolf Volcano, Galápagos Archipelago: Melting and Magmatic Evolution at the Margins of a Mantle Plume. *Journal of Petrology* 46, 2197–2224. https://doi.org/10.1093/petrology/egi052

Geist, D.J., Fornari, D.J., Kurz, M.D., Harpp, K.S., Soule, S.A., Perfit, M.R., Koleszar, A.M. (2006) Submarine Fernandina: Magmatism at the leading edge of the Galápagos hot spot. *Geochemistry, Geophysics, Geosystems* 7, Q12007. https://doi.org/10.1029/2006GC001290

Gibson, S.A., Geist, D. (2010) Geochemical and geophysical estimates of lithospheric thickness variation beneath Galápagos. *Earth and Planetary Science Letters* 300, 275–286. https://doi.org/10.1016/j.epsl.2010.10.002

Gibson, S.A., Geist, D.G., Day, J.A., Dale, C.W. (2012) Short wavelength heterogeneity in the Galápagos plume: Evidence from compositionally diverse basalts on Isla Santiago. *Geochemistry, Geophysics, Geosystems* 13, Q09007. https://doi.org/10.1029/2012GC004244

Gibson, S.A., Dale, C.W., Geist, D.J., Day, J.A., Brügmann, G., Harpp, K.S. (2016) The influence of melt flux and crustal processing on Re–Os isotope systematics of ocean island basalts: Constraints from Galápagos. *Earth and Planetary Science Letters* 449, 345–359. https://doi.org/10.1016/j.epsl.2016.05.021

Haack, U.K. (1969) Spurenelemente in Biotiten aus Graniten und Gneisen. *Contributions to Mineralogy and Petrology* 22, 83–126. https://doi.org/10.1007/BF00372399

Hegner, E., Alexeiev, D.V, Messling, N., Tolmacheva, T.Yu., Willbold, M. (2022) Cambrian-Ordovician mid-ocean ridge magmatism in the Kyrgyz Middle Tianshan and origin of the Karaterek ophiolite. *Lithos* 410–411, 106576. https://doi.org/10.1016/j.lithos.2021.106576

Handley, H.K., Turner, S., Berlo, K., Beier, C., Saal, A.E. (2011) Insights into the Galápagos plume from uranium-series isotopes of recently erupted basalts. *Geochemistry, Geophysics, Geosystems* 12, Q0AC14. https://doi.org/10.1029/2011GC003676

Harpp, K.S., Weis, D. (2020) Insights Into the Origins and Compositions of Mantle Plumes: A Comparison of Galápagos and Hawai'i. *Geochemistry, Geophysics, Geosystems* 21, e2019GC008887. https://doi.org/10.1029/2019GC008887

Harpp, K.S., Fornari, D.J., Geist, D.J., Kurz, M.D. (2003) Genovesa Submarine Ridge: A manifestation of plume-ridge interaction in the northern Galápagos Islands. *Geochemistry, Geophysics, Geosystems* 4, 8511. https://doi.org/10.1029/2003GC000531

Hoernle, K., Abt, D.L., Fischer, K.M., Nichols, H., Hauff, F., *et al.* (2008) Arc-parallel flow in the mantle wedge beneath Costa Rica and Nicaragua. *Nature* 451, 1094–1097. https://doi.org/10.1038/nature06550

Jansen, M.W., Tusch, J., Münker, C., Bragagni, A., Avanzinelli, R., Mastroianni, F., Stuart, F.M., Kurzweil, F. (2022) Upper mantle control on the W isotope record of shallow level plume and intraplate volcanic settings. *Earth and Planetary Science Letters* 585, 117507. https://doi.org/10.1016/j.epsl.2022.117507

Jochum, K.P., Weis, U., Schwager, B., Stoll, B., Wilson, S.A., Haug, G.H., Andreae, M.O., Enzweiler, J. (2016) Reference Values Following ISO Guidelines for Frequently Requested Rock Reference Materials. *Geostandards and Geoanalytical Research* 40, 333–350. https://doi.org/10.1111/j.1751-908X.2015.00392.x

Kessel, R., Schmidt, M.W., Ulmer, P., Pettke, T. (2005) Trace element signature of subduction-zone fluids, melts and supercritical liquids at 120–180 km depth. *Nature* 437, 724–727. https://doi.org/10.1038/nature03971

Kirchenbaur, M., Münker, C. (2015) The behaviour of the extended HFSE group (Nb, Ta, Zr, Hf, W, Mo) during the petrogenesis of mafic K-rich lavas: The Eastern Mediterranean case. *Geochimica et Cosmochimica Acta* 165, 178–199. https://doi.org/10.1016/j.gca.2015.05.030

König, S., Münker, C., Schuth, S., Garbe-Schönberg, D. (2008) Mobility of tungsten in subduction zones. *Earth and Planetary Science Letters* 274, 82–92. https://doi.org/10.1016/j.epsl.2008.07.002

König, S., Münker, C., Hohl, S., Paulick, H., Barth, A.R., Lagos, M., Pfänder, J., Büchl, A. (2011) The Earth's tungsten budget during mantle melting and crust formation. *Geochimica et Cosmochimica Acta* 75, 2119–2136. https://doi.org/10.1016/j.gca.2011.01.031

Kruijer, T.S., Kleine, T. (2018) No ^{182}W excess in the Ontong Java Plateau source. *Chemical Geology* 485, 24–31. https://doi.org/10.1016/j.chemgeo.2018.03.024

Kurzweil, F., Münker, C., Grupp, M., Braukmüller, N., Fechtner, L., Christian, M., Hohl, S.V., Schoenberg, R. (2019) The stable tungsten isotope composition of modern igneous reservoirs. *Geochimica et Cosmochimica Acta* 251, 176–191. https://doi.org/10.1016/j.gca.2019.02.025

Leeman, W.P., Carr, M.J., Morris, J.D. (1994) Boron geochemistry of the Central American Volcanic Arc: Constraints on the genesis of subduction-related magmas. *Geochimica et Cosmochimica Acta* 58, 149–168. https://doi.org/10.1016/0016-7037(94)90453-7

Mazza, S.E., Stracke, A., Gill, J.B., Kimura, J.-I., Kleine, T. (2020) Tracing dehydration and melting of the subducted slab with tungsten isotopes in arc lavas. *Earth and Planetary Science Letters* 530, 115942. https://doi.org/10.1016/j.epsl.2019.115942

Mei, Q.-F., Yang, J.-H., Yang, Y.-H. (2018) An improved extraction chromatographic purification of tungsten from a silicate matrix for high precision isotopic measurements using MC-ICPMS. *Journal of Analytical Atomic Spectrometry* 33, 569–577. https://doi.org/10.1039/C8JA00024G

Palme, H., O'Neill, H.St.C. (2014) 3.1 - Cosmochemical Estimates of Mantle Composition. In: Holland, H.D., Turekian, K.K. (Eds.) *Treatise on Geochemistry*. Second Edition, Elsevier, Amsterdam, 1–39 https://doi.org/10.1016/B978-0-08-095975-7.00201-1

Patino, L.C., Carr, M.J., Feigenson, M.D. (2000) Local and regional variations in Central American arc lavas controlled by variations in subducted sediment input. *Contributions to Mineralogy and Petrology* 138, 265–283. https://doi.org/10.1007/s004100050562

Peterson, M.E., Saal, A.E., Nakamura, E., Kitagawa, H., Kurz, M.D., Koleszar, A.M. (2014) Origin of the 'Ghost Plagioclase' Signature in Galapagos Melt Inclusions: New Evidence from Pb Isotopes. *Journal of Petrology* 55, 2193–2216. https://doi.org/10.1093/petrology/egu054

Peterson, M.E., Saal, A.E., Kurz, M.D., Hauri, E.H., Blusztajn, J.S., Harpp, K.S., Werner, R., Geist, D.J. (2017) Submarine Basaltic Glasses from the Galapagos Archipelago: Determining the Volatile Budget of the Mantle Plume. *Journal of Petrology* 58, 1419–1450. https://doi.org/10.1093/petrology/egx059

Plank, T., Langmuir, C.H. (1998) The chemical composition of subducting sediment and its consequences for the crust and mantle. *Chemical Geology* 145, 325–394. https://doi.org/10.1016/S0009-2541(97)00150-2

Salters, V.J.M., Stracke, A. (2004) Composition of the depleted mantle. *Geochemistry ,Geophysics, Geosystems* 5, Q05B07. https://doi.org/10.1029/2003GC000597

Stubbs, D., Yang, R., Coath, C.D., John, T., Elliott, T. (2022) Tungsten isotopic fractionation at the Mariana arc and constraints on the redox conditions of subduction zone fluids. *Geochimica et Cosmochimica Acta* 334, 135–154. https://doi.org/10.1016/j.gca.2022.08.005

Tappe, S., Budde, G., Stracke, A., Wilson, A., Kleine, T. (2020) The tungsten-182 record of kimberlites above the African superplume : Exploring links to the core-mantle boundary. *Earth and Planetary Science Letters* 547, 116473. https://doi.org/10.1016/j.epsl.2020.116473

Tusch, J., Sprung, P., van de Löcht, J., Hoffmann, J.E., Boyd, A.J., Rosing, M.T., Münker, C. (2019) Uniform ^{182}W isotope compositions in Eoarchean rocks from the Isua region, SW Greenland: The role of early silicate differentiation and missing late veneer. *Geochimica et Cosmochimica Acta* 257, 284–310. https://doi.org/10.1016/j.gca.2019.05.012

Tusch, J., Hoffmann, J.E., Hasenstab, E., Fischer-Gödde, M., Marien, C.S., Wilson, A.H., Münker, C. (2022) Long-term preservation of Hadean protocrust in Earth's mantle. *Proceedings of the National Academy of Sciences* 119, e2120241119. https://doi.org/10.1073/pnas.2120241119

Völkening, J., Köppe, M., Heumann, K.G. (1991) Tungsten isotope ratio determinations by negative thermal ionization mass spectrometry. *International Journal of Mass Spectrometry and Ion Processes* 107, 361–368. https://doi.org/10.1016/0168-1176(91)80070-4

Wegner, W., Wörner, G., Harmon, R.S., Jicha, B.R. (2011) Magmatic history and evolution of the Central American Land Bridge in Panama since Cretaceous times. *Bulletin of the Geological Society of America* 123, 703–724. https://doi.org/10.1130/B30109.1

Werner, R., Hoernle, K., Barckhausen, U., Hauff, F. (2003) Geodynamic evolution of the Galápagos hot spot system (Central East Pacific) over the past 20 m.y.: Constraints from morphology, geochemistry, and magnetic anomalies. *Geochemistry, Geophysics, Geosystems* 4, 1108. https://doi.org/10.1029/2003GC000576

White, W.M., McBirney, A.R., Duncan, R.A. (1993) Petrology and geochemistry of the Galápagos Islands: Portrait of a pathological mantle plume. *Journal of Geophysical Research: Solid Earth* 98, 19533–19563. https://doi.org/10.1029/93JB02018

Willbold, M., Elliott, T., Moorbath, S. (2011) The tungsten isotopic composition of the Earth's mantle before the terminal bombardment. *Nature* 477, 195–198. https://doi.org/10.1038/nature10399

Wörner, G., Harmon, R.S., Wegner, W. (2009) Geochemical evolution of igneous rocks and changing magma sources during the formation and closure of the Central American land bridge of Panama. In: Kay, S.M., Ramos, V.A., Dickinson, W.R. (Eds.) *Backbone of the Americas: Shallow Subduction, Plateau Uplift, and Ridge and Terrane Collision.* GSA Memoir 204, Geological Society of America, Boulder, 183–196. https://doi.org/10.1130/2009.1204(08)